SUPPLEMENTAL DATA

SUPPLEMENTAL TABLES

Table S1. Structures of DNA probes used.

1. [-59/+21], N25cons promoter

CGCTAAAATTTTTTTTAAAAGTAT**TTGACA**TCAGGAAAATTTTT**TG**G**TATAAT**AGATTC**A**TAAATTTGAGAGAGGAGTTT
GCGATTTTAAAAAAAATTTTCATA**AACTGT**AGTCCTTTTAAAAA**AC**C**ATATTA**TCTAAG**T**ATTTAAACTCTCTCCTCAAA

2. [-59/+14]

CGCTAAAATTTTTTTTAAAAGTAT**TTGACA**TCAGGAAAATTTTT**TG**G**TATAAT**AGATTC**A**TAAATTTGAGAGA
GCGATTTTAAAAAAAATTTTCATA**AACTGT**AGTCCTTTTAAAAA**AC**C**ATATTA**TCTAAG**T**ATTTAAACTCTCT

3. [-59/+8]

CGCTAAAATTTTTTTTAAAAGTAT**TTGACA**TCAGGAAAATTTTT**TG**G**TATAAT**AGATTC**A**TAAATTT
GCGATTTTAAAAAAAATTTTCATA**AACTGT**AGTCCTTTTAAAAA**AC**C**ATATTA**TCTAAG**T**ATTTAAA

4. [-59/+7]

CGCTAAAATTTTTTTTAAAAGTAT**TTGACA**TCAGGAAAATTTTT**TG**G**TATAAT**AGATTC**A**TAAATT
GCGATTTTAAAAAAAATTTTCATA**AACTGT**AGTCCTTTTAAAAA**AC**C**ATATTA**TCTAAG**T**ATTTAA

5. [-59/+6]

CGCTAAAATTTTTTTTAAAAGTAT**TTGACA**TCAGGAAAATTTTT**TG**G**TATAAT**AGATTC**A**TAAAT
GCGATTTTAAAAAAAATTTTCATA**AACTGT**AGTCCTTTTAAAAA**AC**C**ATATTA**TCTAAG**T**ATTTA

6. [-59/+5]

CGCTAAAATTTTTTTTAAAAGTAT**TTGACA**TCAGGAAAATTTTT**TG**G**TATAAT**AGATTC**A**TAAA
GCGATTTTAAAAAAAATTTTCATA**AACTGT**AGTCCTTTTAAAAA**AC**C**ATATTA**TCTAAG**T**ATTT

7. [-59/+4]

CGCTAAAATTTTTTTTAAAAGTAT**TTGACA**TCAGGAAAATTTTT**TG**G**TATAAT**AGATTC**A**TAA
GCGATTTTAAAAAAAATTTTCATA**AACTGT**AGTCCTTTTAAAAA**AC**C**ATATTA**TCTAAG**T**ATT

8. [-59/+3]

CGCTAAAATTTTTTTTAAAAGTAT**TTGACA**TCAGGAAAATTTTT**TG**G**TATAAT**AGATTC**A**TA
GCGATTTTAAAAAAAATTTTCATA**AACTGT**AGTCCTTTTAAAAA**AC**C**ATATTA**TCTAAG**T**AT

9. [-59/+6], +3/+5 = CCG

CGCTAAAATTTTTTTTAAAAGTAT**TTGACA**TCAGGAAAATTTTT**TG**G**TATAAT**AGATTC**A**TCCGT
GCGATTTTAAAAAAAATTTTCATA**AACTGT**AGTCCTTTTAAAAA**AC**C**ATATTA**TCTAAG**T**AGGCA

10. [-59/+4], +3/+4 = CC

CGCTAAAATTTTTTTTAAAAGTAT**TTGACA**TCAGGAAAATTTTT**TG**G**TATAAT**AGATTC**A**TCC
GCGATTTTAAAAAAAATTTTCATA**AACTGT**AGTCCTTTTAAAAA**AC**C**ATATTA**TCTAAG**T**AGG

11. [-59/+6], +3/+6 = CGCG

CGCTAAAATTTTTTTTAAAAGTAT**TTGACA**TCAGGAAAATTTTT**TG**G**TATAAT**AGATTC**A**TCGCG
GCGATTTTAAAAAAAATTTTCATA**AACTGT**AGTCCTTTTAAAAA**AC**C**ATATTA**TCTAAG**T**AGCGC

12. [-59/+4], +3/+4 = CG

CGCTAAAATTTTTTTTAAAAGTAT**TTGACA**TCAGGAAAATTTTT**TG**G**TATAAT**AGATTC**A**TCG
GCGATTTTAAAAAAAATTTTCATA**AACTGT**AGTCCTTTTAAAAA**AC**C**ATATTA**TCTAAG**T**AGC

13. [-59/+6], heteroduplex at -3/+1

CGCTAAAATTTTTTTTAAAAGTAT**TTGACA**TCAGGAAAATTTTT**TG**G**TATAAT**AGACCT**T**TAAAT
GCGATTTTAAAAAAAATTTTCATA**AACTGT**AGTCCTTTTAAAAA**AC**C**ATATTA**TCTAAG**T**ATTTA

14. [-59/+4], heteroduplex at -3/+1

CGCTAAAATTTTTTTTAAAAGTAT**TTGACA**TCAGGAAAATTTTT**TG**G**TATAAT**AGACCT**T**TAA
GCGATTTTAAAAAAAATTTTCATA**AACTGT**AGTCCTTTTAAAAA**AC**C**ATATTA**TCTAAG**T**ATT

15. [-59/-5/+21]

CGCTAAAATTTTTTTTAAAAGTAT**TTGACA**TCAGGAAAATTTTT**TG**G**TATAAT**AG
GCGATTTTAAAAAAAATTTTCATA**AACTGT**AGTCCTTTTAAAAA**AC**C**ATATTA**TCTAAG**T**ATTTAAACTCTCTCCTCAAA

16. [-59/-5/+8]

CGCTAAAATTTTTTTTAAAAGTAT**TTGACA**TCAGGAAAATTTTT**TG**G**TATAAT**AG
GCGATTTTAAAAAAAATTTTCATA**AACTGT**AGTCCTTTTAAAAA**AC**C**ATATTA**TCTAAG**T**ATTTAAA

17. [-59/-5/+6]

CGCTAAAATTTTTTTTAAAAGTAT**TTGACA**TCAGGAAAATTTTT**TG**G**TATAAT**AG
GCGATTTTAAAAAAAATTTTCATA**AACTGT**AGTCCTTTTAAAAA**AC**C**ATATTA**TCTAAG**T**ATTTA

18. [-59/-5/+5]

CGCTAAAATTTTTTTTAAAAGTATTTGACATCAGGAAAATTTTTTGGTATAATAG
GCGATTTTAAAAAAAATTTTCATAAACTGTAGTCCTTTTAAAAAACCATATTATCTAAGTATTT

19. [-59/-5/+4]

CGCTAAAATTTTTTTTAAAAGTATTTGACATCAGGAAAATTTTTTGGTATAATAG
GCGATTTTAAAAAAAATTTTCATAAACTGTAGTCCTTTTAAAAAACCATATTATCTAAGTATT

20. [-59/+31], break between +6/+7 positions of the template strand

CGCTAAAATTTTTTTTAAAAGTATTTGACATCAGGAAAATTTTTTGGTATAATAGATTCATAAATTTGAGAGAGGAGTTTAAATATGGCT
GCGATTTTAAAAAAAATTTTCATAAACTGTAGTCCTTTTAAAAAACCATATTATCTAAGTATTTAAACTCTCTCCTCAAATTTATACCGA

21. [-59/+31], break between +4/+5 positions of the template strand

CGCTAAAATTTTTTTTAAAAGTATTTGACATCAGGAAAATTTTTTGGTATAATAGATTCATAAATTTGAGAGAGGAGTTTAAATATGGCT
GCGATTTTAAAAAAAATTTTCATAAACTGTAGTCCTTTTAAAAAACCATATTATCTAAGTATTTAAACTCTCTCCTCAAATTTATACCGA

22. [-59/+21], -2/-4= CCG

CGCTAAAATTTTTTTTAAAAGTATTTGACATCAGGAAAATTTTTTGGTATAATAGCCGCATAAATTTGAGAGAGGAGTTT
GCGATTTTAAAAAAAATTTTCATAAACTGTAGTCCTTTTAAAAAACCATATTATCGGCGTATTTAAACTCTCTCCTCAAA

23. [-59/+14], -2/-4= CCG

CGCTAAAATTTTTTTTAAAAGTATTTGACATCAGGAAAATTTTTTGGTATAATAGCCGCATAAATTTGAGAGA
GCGATTTTAAAAAAAATTTTCATAAACTGTAGTCCTTTTAAAAAACCATATTATCGGCGTATTTAAACTCTCT

24. [-59/+10], -2/-4= CCG

CGCTAAAATTTTTTTTAAAAGTATTTGACATCAGGAAAATTTTTTGGTATAATAGCCGCATAAATTTGA
GCGATTTTAAAAAAAATTTTCATAAACTGTAGTCCTTTTAAAAAACCATATTATCGGCGTATTTAAACT

25. [-59/+8], -2/-4= CCG

CGCTAAAATTTTTTTTAAAAGTATTTGACATCAGGAAAATTTTTTGGTATAATAGCCGCATAAATTT
GCGATTTTAAAAAAAATTTTCATAAACTGTAGTCCTTTTAAAAAACCATATTATCGGCGTATTTAAA

26. [-59/+6], -2/-4= CCG

CGCTAAAATTTTTTTTAAAAGTATTTGACATCAGGAAAATTTTTTGGTATAATAGCCGCATAAAT
GCGATTTTAAAAAAAATTTTCATAAACTGTAGTCCTTTTAAAAAACCATATTATCGGCGTATTTA

27. [-59/+4], -2/-4= CCG

CGCTAAAATTTTTTTTAAAAGTATTTGACATCAGGAAAATTTTTTGGTATAATAGCCGCATAA
GCGATTTTAAAAAAAATTTTCATAAACTGTAGTCCTTTTAAAAAACCATATTATCGGCGTATT

28. [-58/-14], competitor probe

GCTAAAATTTTTTTTAAAAGTATTTGACATCAGGAAAATTTTTTG
CGATTTTAAAAAAAATTTTCATAAACTGTAGTCCTTTTAAAAAAC

29. [-62/+21], λPr promoter, -12T

AGGGATAAATATCTAACACCGTGCGTGTTGACTATTTTACCTCTGGCGGTTATAATGGTTGCATGTACTAAGGAGGTTGTATG
TCCCTATTTATAGATTGTGGCACGCACAACTGATAAAATGGAGACCGCCAATATTACCAACGTACATGATTCCTCCAACATAC

30. [-62/+10]

AGGGATAAATATCTAACACCGTGCGTGTTGACTATTTTACCTCTGGCGGTTATAATGGTTGCATGTACTAAG
TCCCTATTTATAGATTGTGGCACGCACAACTGATAAAATGGAGACCGCCAATATTACCAACGTACATGATTC

31. [-62/+6]

AGGGATAAATATCTAACACCGTGCGTGTTGACTATTTTACCTCTGGCGGTTATAATGGTTGCATGTAC
TCCCTATTTATAGATTGTGGCACGCACAACTGATAAAATGGAGACCGCCAATATTACCAACGTACATG

32. [-62/+4]

AGGGATAAATATCTAACACCGTGCGTGTTGACTATTTTACCTCTGGCGGTTATAATGGTTGCATGT
TCCCTATTTATAGATTGTGGCACGCACAACTGATAAAATGGAGACCGCCAATATTACCAACGTACA

33. [-38/-11/-12], upstream fork junction

TATTTGACATCAGGAAAATTTTTTGGTA
ATAAACTGTAGTCCTTTTAAAAAACCA

34. [-38/-9/-12], upstream fork junction

TATTTGACATCAGGAAAATTTTTCTGTATA
ATAAACTGTAGTCCTTTTAAAAAGACA

35. [-11/+16/+2], downstream fork junction

ATAATAGATTCATAAATTTGAGAGAGG
ATTTAAACTCTCTCC

36. [-11/+16/+2], -8T substituted downstream fork junction

ATATTAGATTCATAAATTTGAGAGAGG
ATTTAAACTCTCTCC

37. -11+2 oligo

ATAATAGATTCAT

The probe numbers and abbreviations used in the text are shown above the sequences. The -10 and -35 promoter element sequences are highlighted in larger size font, the start site (+1) position is underlined. Substituted nucleotides are shown in red. Numbers in brackets correspond to borders of strands of probes with respect to the transcription start position (+1).

Table S2. Abortive transcription activity from duplex N25cons derivatives sharply decreases upon moving the downstream edge of the duplex from +6 to +4 positions.

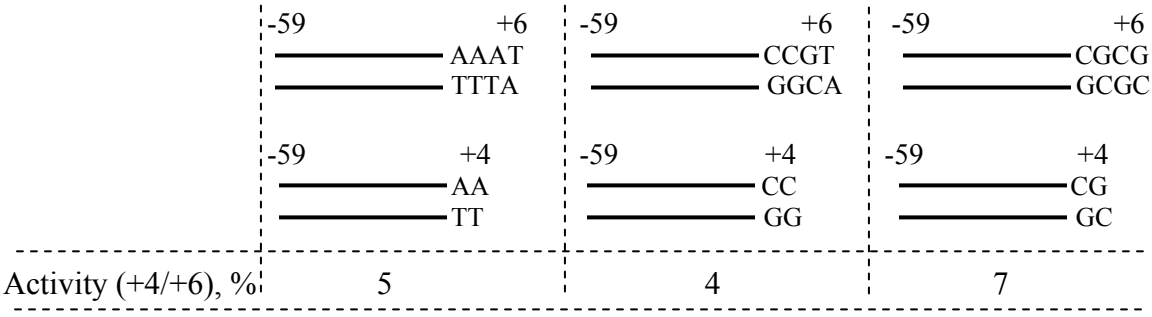

Activities of probes 5, 9, 11 with downstream edges at +4 relative to activities of corresponding probes 7, 10, 12 extended to +6 are shown. The full sequences of the probes are shown in Table S1.

SUPPLEMENTAL FIGURES

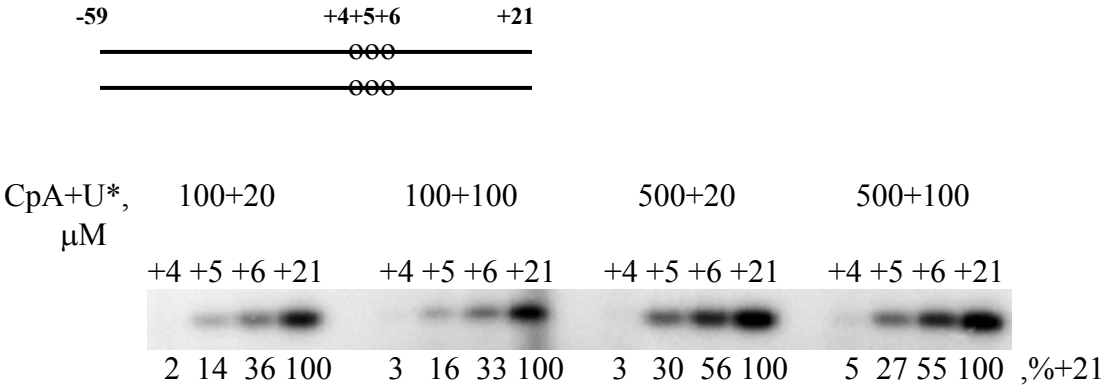

Figure S1. Abortive transcript synthesis from duplex N25cons derivatives (probes 1, 5-7) at various nucleotide concentrations.

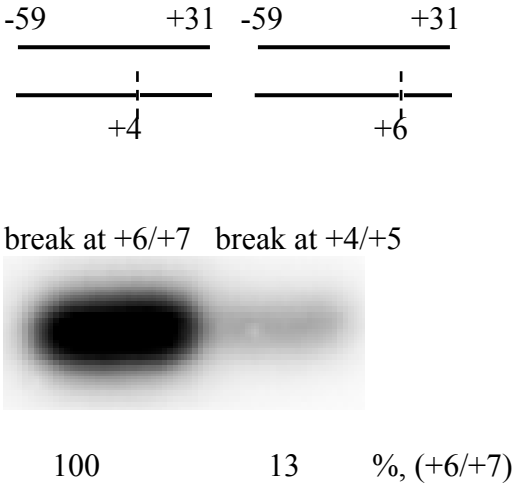

Figure S2. Abortive transcript synthesis from discontinuous N25cons derivatives (probes 20, 21) that lacked a phosphate group between either +4/+5 or +6/+7 positions of the template strand.

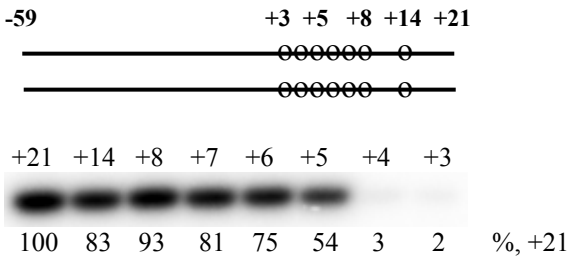

Figure S3. Abortive transcript synthesis from duplex N25cons derivatives (probes 1-8) by RNAP reconstituted with σ^{70} deleted for region 1.1.

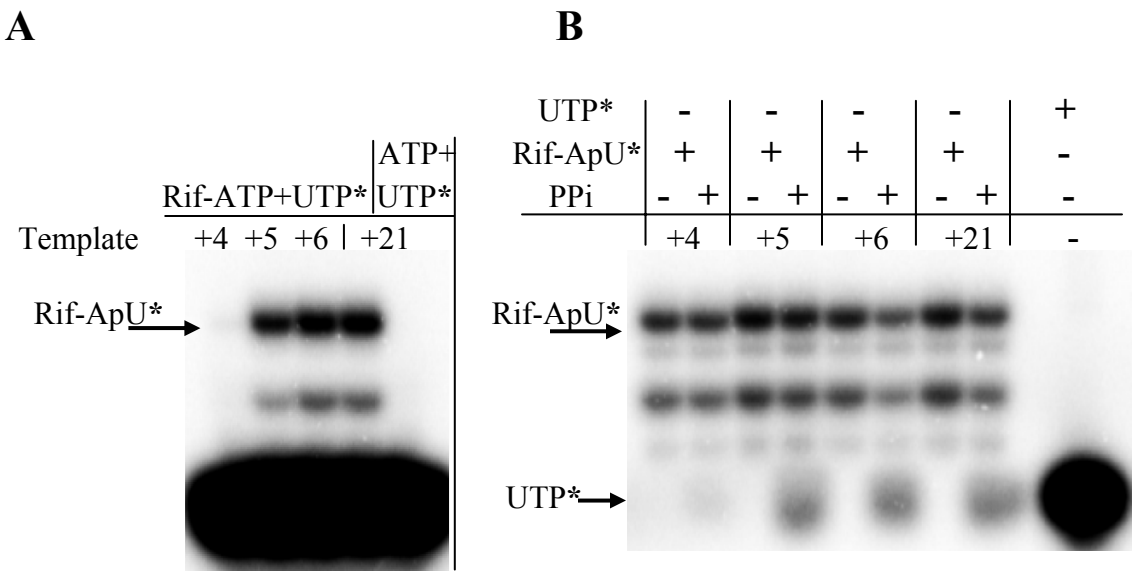

Figure S4. Measuring of transcription initiation and pyrophosphorolysis using a chimeric rifampicin-ATP compound as a primer.

(A) Abortive transcript synthesis from duplex N25cons derivatives with downstream edges at +21, +6, +5, and +4 (probes 1, 5-7) using Rif-ATP (2 μM) as a primer. ATP (2 μM) was used as a primer instead of Rif-ATP in a control reaction shown in last lane. (B) Pyrophosphorolysis of Rif-ApU in RNAP complexes with duplex N25cons derivatives. Pyrophosphate concentration was 0.5 mM.

Two products were formed in the course of the synthesis reactions (Fig. S4A). Relative amount of the higher mobility product further increased during the Rif-ApU extraction performed under rather harsh conditions (compare intensities of the higher mobility product bands in Fig. S4A and B). Therefore, we think that the higher mobility band may correspond to a product of Rif-ApU decomposition.

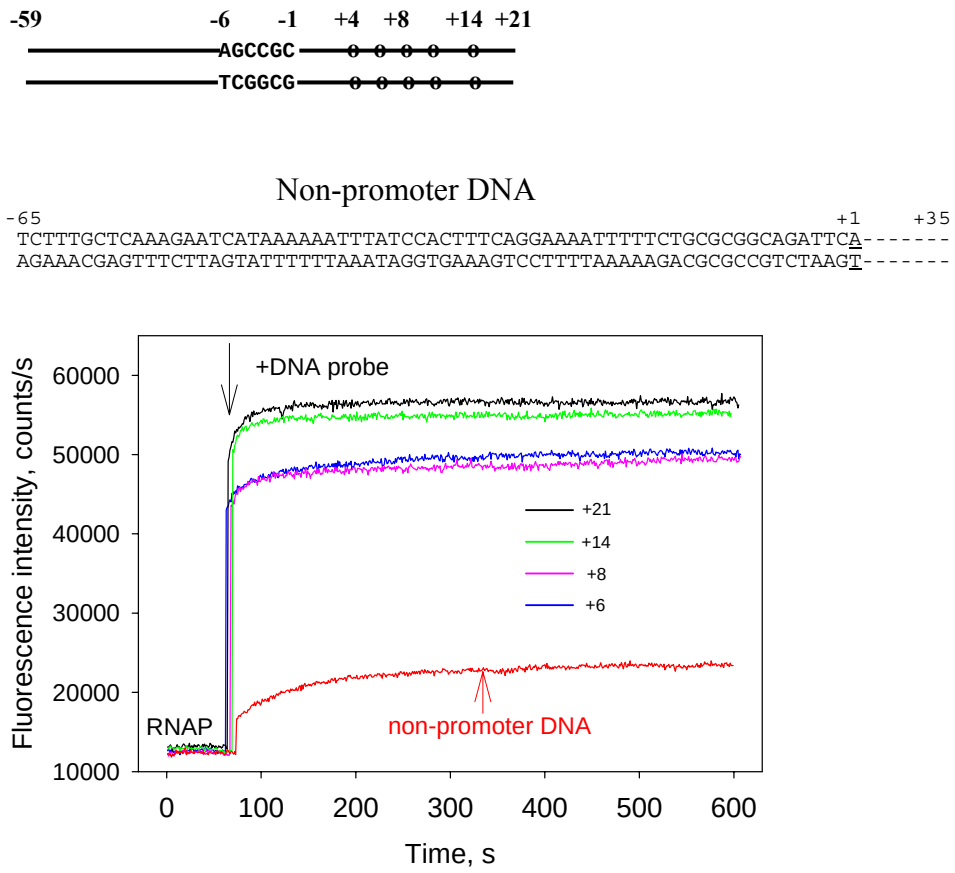

Figure S5. Measuring of RNAP interactions with bearing G+C rich discriminator derivatives of N25cons using the RNAP beacon assay. Time dependence of the increase in fluorescence upon mixing 1 nM RNAP beacon with 2 nM DNA probes 22, 23, 25, 26 whose downstream end positions (+21, +14, +8 and +6, respectively) are indicated in the panel, and with 2 nM control non-promoter DNA. Non-promoter DNA template shown above the panel is based on T5N25 promoter sequence but contains multiple substitutions in the −35 and −10 regions and lacks transcription activity in vitro (12).

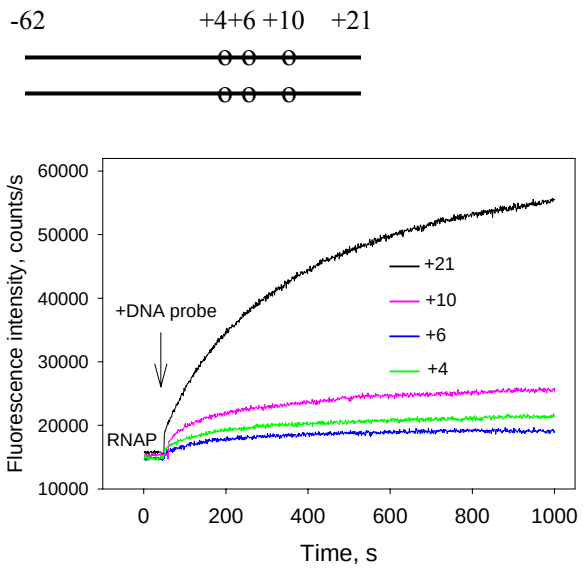

Figure S6. Measuring of RNAP interactions with derivatives of λPr promoter using the RNAP beacon assay. Time dependence of the increase in fluorescence upon mixing 1 nM RNAP beacon with 2 nM indicated λPr derivatives whose downstream ends were located at +21,+10,+6, and +4 (probes 29-32).

A

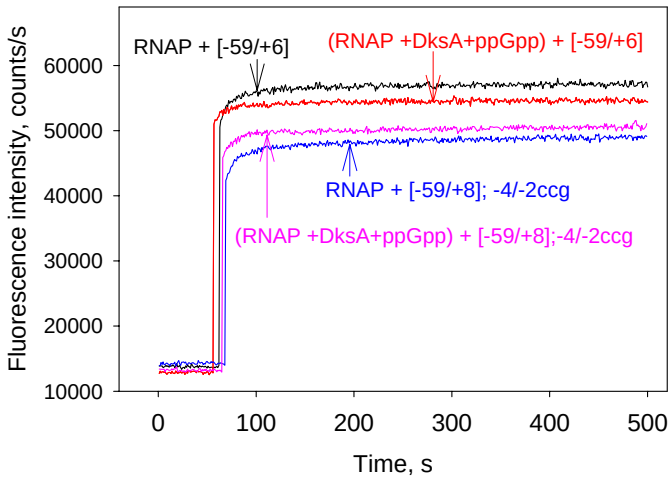
RNAP + [-59/+6]
(RNAP +DksA+ppGpp) + [-59/+6]
RNAP + [-59/+8]; -4/-2ccg
(RNAP +DksA+ppGpp) + [-59/+8];-4/-2ccg
Fluorescence intensity, counts/s
Time, s

B

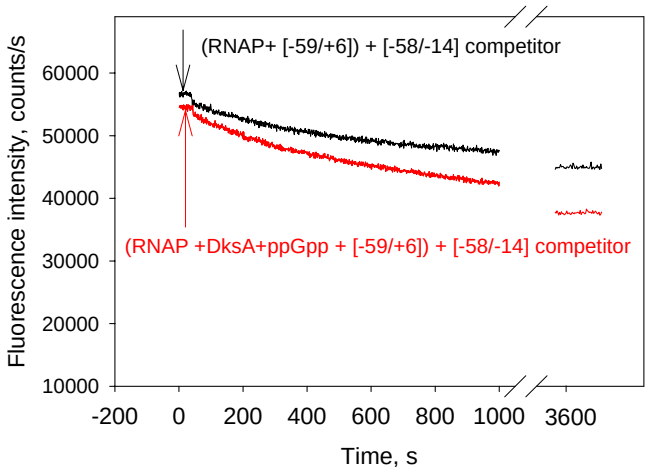
(RNAP+ [-59/+6]) + [-58/-14] competitor
(RNAP +DksA+ppGpp + [-59/+6]) + [-58/-14] competitor
Fluorescence intensity, counts/s
Time, s

C

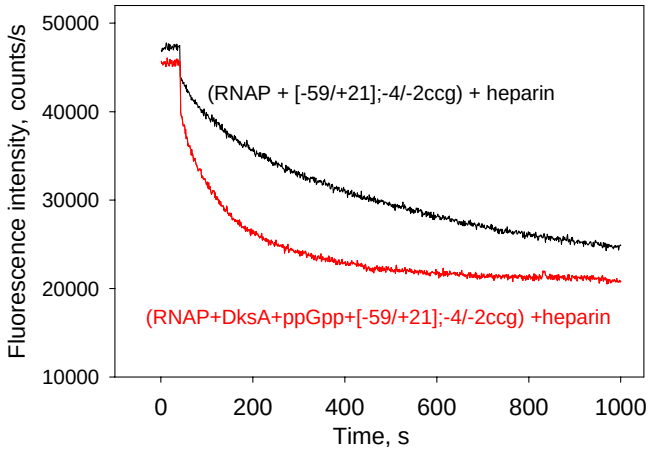
(RNAP + [-59/+21];-4/-2ccg) + heparin
(RNAP+DksA+ppGpp+[-59/+21];-4/-2ccg) +heparin
Fluorescence intensity, counts/s
Time, s

Figure S7. Measuring of RNAP interactions with duplex probes in the absence or presence of DksA and ppGpp. (A) Time dependences of the increase in fluorescence upon mixing 1 nM RNAP beacon with 2 nM [-59/+6] (probe 5) or 2nM [-59/+8];-4/-2ccg (probe 25), in the absence or presence of 2 μM DksA and 100 μM ppGpp. (B) Time-dependent changes of the fluorescence signal were measured upon the addition of 2 nM [-58/-14] competitor to RNAP beacon complexes with [-59/+6] which were preformed in the absence or presence of 2 μM DksA and 100 μM ppGpp. (C) Time-dependent changes of the fluorescence signal were measured upon the addition of 20 μg/ml heparin to RNAP beacon complexes with [-59/+21];-4/-2ccg probe (probe 22) which were preformed in the absence or presence of 2 μM DksA and 100 μM ppGpp.

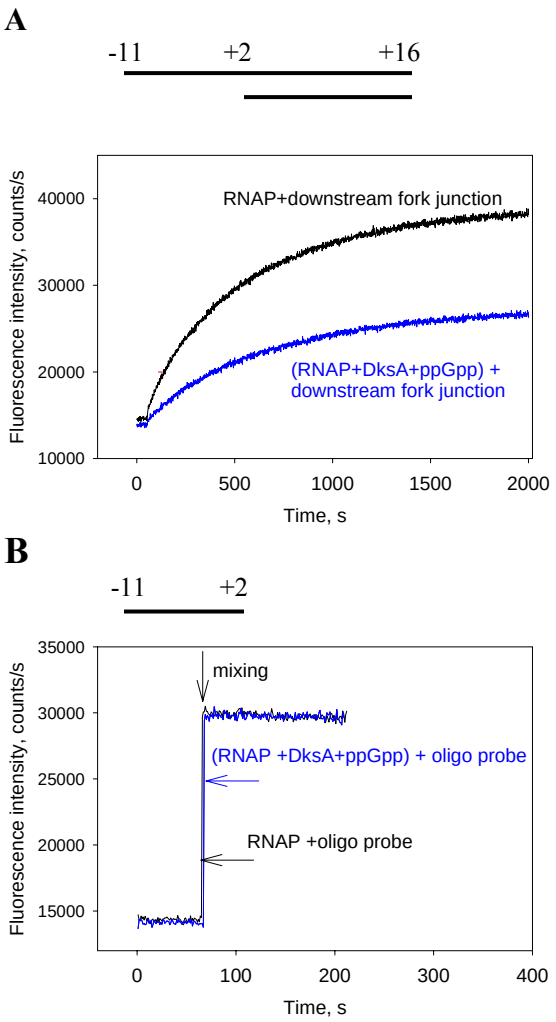

Figure S8. DksA and ppGpp affect RNAP binding to downstream fork junction probe and does not influence RNAP binding to oligonucleotide probe. (A) Black curve, time dependence of the increase in fluorescence upon mixing 1 nM RNAP beacon with 2 nM downstream fork junction (probe 35). Blue curve, same as black curve, but RNAP beacon was preincubated with 2 μM DksA and 100 μM ppGpp for 2 min prior to the addition of downstream fork junction. (B) Black curve, time dependence of the increase in fluorescence upon mixing 1 nM RNAP beacon with 200 nM -11+2 oligo (probe 37). Blue curve, same as black curve, but RNAP beacon was preincubated with 2

μM DksA and 100 μM ppGpp for 2 min prior to the addition of downstream fork junction.

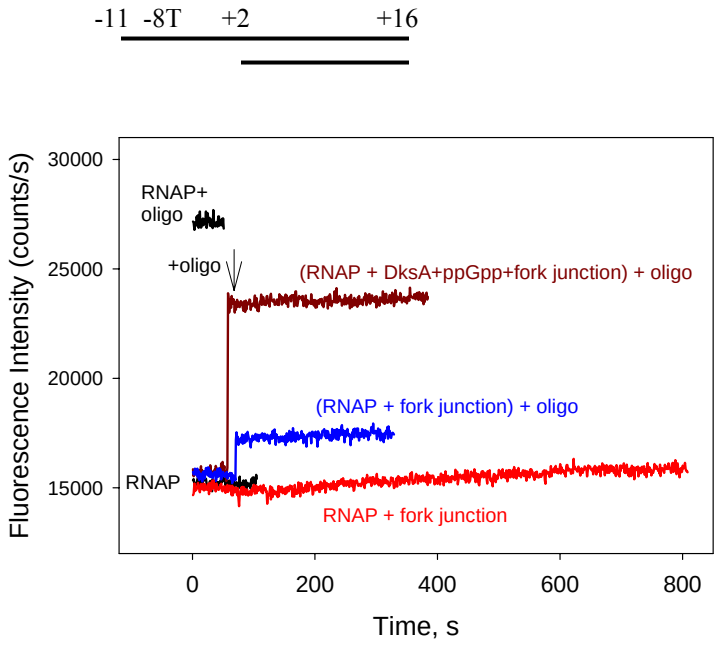

Figure S9. RNAP beacon assay for RNAP occupancy by downstream fork junction. Time-dependent change of the fluorescence signal upon addition of 200 nM -11/+2 oligo to samples containing 1 nM RNAP beacon preincubated with 2nM of -8T substituted downstream fork junctions (probe 36) for 1 hour in the absence or presence of 2 μM DksA and 100 μM ppGpp (curves "(RNAP+fork junction)+oligo" and "(RNAP + DksA + ppGpp + fork junction) + oligo", respectively. Fluorescence signal measured with free RNAP beacon and signals measured upon addition of the oligo or fork junction to RNAP beacon are indicated as "RNAP", "RNAP + oligo" and "RNAP + fork junction", respectively. A more detailed explanation of the experiment follows.

The dissociation constants (K_d) of RNAP complex with downstream fork junction probe 36 shown in Table S1 were determined essentially as in (9), in the absence and presence of DksA and ppGpp. The beacon fluorescent signals generated by -8T substituted downstream fork junctions are low (Fig. S9, also see Ref. (9)), which hinders calculation of K_d from dependence of the fluorescent signal amplitude on DNA probe concentration. Affinity of RNAP beacon to this probe was evaluated by a competition binding assay using -11/+2 oligo (probe 37) as a competitor. Figure S9 shows changes in florescence intensity after addition of 200 nM -11/+2 oligo to free RNAP beacon and to samples in which RNAP beacon was preincubated with 2 nM of the -8T substituted fork junction (probe 36) for 1 hour, in the absence or presence of 2 μM DksA and 100μM ppGpp. Upon the addition of -11/+2 to free RNAP beacon, the signal increased and reached saturation intensity for a few seconds (see Fig. S8B). Upon similar oligo addition to the samples containing fork junction, a rapid increase in the signal intensity was followed by very slow change of the signal. The initial fast intensity increase in the samples containing fork junction apparently corresponds to oligo interaction with free RNAP beacon molecules, while the slow kinetics reflects reaching of equilibrium between the oligo and bound to RNAP fork junctions. Consequently, amplitude of the rapid increase is proportional to concentration of RNAP beacons remained unbound to fork junctions before the oligo addition. Therefore, occupancy (X) of RNAP beacon by a fork junction probe was determined as $X = 1-I/I_0$, where I_0 is amplitude of the oligo signal measured with free beacon and I is amplitude of the rapid increase measured in sample containing beacon preequilibrated with a fork junction. The Kd values were calculated from these data by using a chemical equilibrium equation [S1].

(1-X)(C-[RNAP]X) = K_d X, [S1]

where C is fork junction concentration.

The RNAP occupancies and calculated K_d values are shown in Fig. 5B.

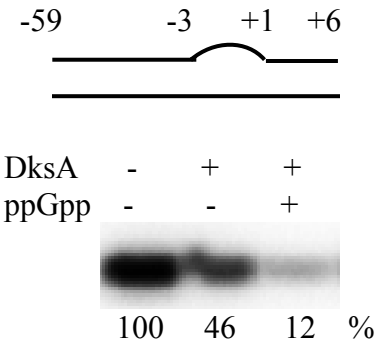

Figure S10. The effect of DksA and ppGpp on abortive transcript synthesis from probe 13 containing a mismatched segment spanning positions -3 to +1.